

Impaired Hepatic Regeneration in Metallothionein-I/II Knockout Mice After Partial Hepatectomy

JORDAN R. OLIVER, TOM W. MARA, AND M. GEORGE CHERIAN¹

Department of Pathology, Faculty of Medicine and Dentistry, University of Western Ontario, London, Ontario, Canada N6A 5C1

Although the translocation of metallothionein (MT) from cytoplasm to nucleus has been demonstrated in liver during times of high requirement for zinc (fetal development and the neonatal period), the role of MT in cellular growth is not well understood. In this study, a potential role of MT in liver regeneration was investigated in wild type (WT) and MT-I and MT-II gene knockout (MT-null) mice after 35% partial hepatectomy (PH) or sham laparotomy. Hepatic MT levels and proliferation index were measured at 0, 5, 15, 24, 36, 48, and 60 hrs after PH and 48 hrs after sham laparotomy (control). MT levels were increased in WT mice (peak at 24 hrs after PH) and declined to normal levels by 60 hrs after PH. Immunohistochemical staining for MT in WT mice indicated the presence of MT in both nucleus and cytoplasm of hepatocytes at 24 hrs after PH, whereas MT was present mainly in the cytoplasm at 36–60 hrs after PH and 48 hrs after sham laparotomy. Hepatic proliferation index in both WT and MT-null mice, as determined by argyrophilic nucleolar organizing region staining and proliferating cell nuclear antigen immunohistochemical staining, reached a peak at 48 hrs and declined by 60 hrs after PH. Cell proliferation was significantly less in MT-null mice as compared to WT mice during liver regeneration after PH. These results suggest that MT may play a positive role in hepatic regeneration after PH. *Exp Biol Med* 230:61–67, 2005

Key words: metallothionein; zinc; partial hepatectomy; liver regeneration

Introduction

Unlike many other organs, the liver has a high capacity for regeneration after injury. The rodent liver, for example,

will regenerate 100% of its lost mass within 8 days of surgical resection (1). Liver regeneration is a highly synchronized multistep process consisting of three phases: initiation, proliferation, and termination (2). In the initiation phase, quiescent hepatocytes are primed to respond to growth factors via the action of cytokines, such as tumor necrosis factor α (TNF- α) and interleukin 6 (IL-6). This priming stage marks the transition from G₀ to G₁ stage of the cell cycle, bringing hepatocytes into a state of replicative competence. In the proliferation phase, hepatocytes enter S phase of the cell cycle by stimulation of mitogens such as hepatocyte growth factor (HGF), transforming growth factor α (TGF- α), and epidermal growth factor (EGF). The termination phase is initiated by upregulation of transforming growth factor β (TGF- β) and activin, which suppress epithelial cell growth (3).

Metallothioneins (MTs) are low-molecular weight intracellular proteins involved in many physiological processes, including zinc homeostasis. Among their many putative functions, MTs may play a role in the intracellular storage of zinc. In addition, MTs can donate zinc to zinc finger proteins involved in cellular signaling and transcriptional regulation. *In vitro* studies have shown that MT can supply zinc to the zinc finger transcription factors Sp1, TFIIB, estrogen receptor, and tramtrack (4–7). This reaction may occur by direct donation of zinc from MT through a protein-protein interaction (8). Because of its high thiol content, MT can also function as an antioxidant. *In vitro* studies suggest a direct reaction of hydrogen peroxide with the sulfhydryl groups of MT (9, 10). It has been shown that MT, especially bound to zinc, has a higher capacity to protect against radiation-induced DNA damage than glutathione, another antioxidant (11).

High levels of MT bound to zinc and copper have been detected in liver during fetal development and the neonatal period, when there is a high requirement for zinc in cellular growth (12–14). A transient nuclear localization of MT has been demonstrated in human, rat, and mouse hepatocytes during the fetal/neonatal period (15–17). Studies have shown that MT is induced during liver regeneration, a time of extensive hepatocellular proliferation and high require-

This research was supported by Canadian Institute of Health Research (CIHR) and National Science and Engineering Research Council (NSERC) grants.

¹ To whom correspondence should be addressed at M. George Cherian, Department of Pathology, University of Western Ontario, London, Ontario, Canada N6A 5C1. E-mail: mcherian@uwo.ca

Received August 10, 2004.
Accepted September 17, 2004.

1535-3702/05/2301-0061\$15.00
Copyright © 2005 by the Society for Experimental Biology and Medicine

ment for essential metals such as zinc. Tohyama *et al.* (18) and Tsujikawa *et al.* (19) demonstrated the induction and nuclear localization of MT in rat hepatocytes after partial hepatectomy (PH). Theocharis *et al.* (20) demonstrated the induction of MT in regenerating rat liver after hepatic injury with administration of carbon tetrachloride.

Because there are few studies on the role of MT in cellular growth, this study was undertaken with MT-I and MT-II gene knockout (MT-null) mice to investigate potential roles for MT in liver regeneration after PH. The changes in hepatic proliferation index in wild type (WT) and MT-null mice were compared with argyrophilic nucleolar organizing region (AgNOR) staining and proliferating cell nuclear antigen (PCNA) immunohistochemical staining techniques at different time points after PH. Immunohistochemical staining for MT was used to examine changes in the subcellular localization of MT after PH.

Materials and Methods

Animals and Surgical Procedures. Homozygous MT-I/MT-II null transgenic (129s7/SvEv-Brd-Mt1^{tm1Bri}Mt2^{tm1Bri}) and WT mice (129s3/SvImJ) were obtained from Jackson Laboratories (Bar Harbor, ME) and were bred in the animal facilities at the University of Western Ontario. Animals were housed four per cage and were maintained in a controlled temperature and humidity environment of 12:12-hr light:dark cycles. All animals were fed mouse chow (Harlan Teklad 2018) and water *ad libitum*. PH was performed in 8- to 16-weeks-old male and female mice, as described previously (21) with few modifications. Briefly, mice were anesthetized with an intraperitoneal injection of ketamine (100 mg/kg) and xylazine (5 mg/kg) (K+X), and a midline incision was made. The left lower lobe, comprising approximately 35% of total liver weight, was ligated with a silk suture and resected. The peritoneum was then reapproximated followed by closure of the skin with a running nylon suture. To replace fluid loss from bleeding and fluid shifts the mice were given approximately 0.3 ml sterile saline subcutaneously on the back after closure of the abdomen. Animals were observed postoperatively for pain (vocalization, hunched posture) and were given a subcutaneous injection of buprenorphine (0.07 mg/kg) every 8 hrs, if needed for analgesia. Laparotomized mice, which underwent the same procedure as described above without liver resection, served as sham-operated controls.

Groups of three or six mice were killed at different time points (0, 5, 15, 24, 36, 48, and 60 hrs) after PH or 48 hrs after sham laparotomy, and the liver remnants were removed, weighed, and either frozen at -80°C for MT quantification or processed for histology. For immunohistochemistry and proliferation index determination, liver samples were fixed in 10% formalin overnight and embedded in paraffin. All procedures were performed in accordance with the guidelines of the Canadian Council on Animal Care.

MT Measurement by Cadmium-Hemoglobin

Assay. Hepatic MT levels were determined by a cadmium-hemoglobin (Cd-heme) assay as described previously (22). The method used radioactive ^{109}Cd , and the concentration of MT was calculated in each sample by measurement of ^{109}Cd radioactivity with a gamma counter (1272 Clinigamma, LKB Wallac; Turku, Finland). This was converted to MT concentration on the basis of 7 g-atoms of Cd per molecule of MT. The total hepatic MT concentrations were expressed as micrograms per gram of wet tissue.

AgNOR Staining. Cell proliferation was determined with the AgNOR staining method as described previously (23) with few modifications. Briefly, paraffin-embedded liver samples were sectioned at 3 μm , followed by deparaffinization and rehydration with sequential passes through xylene and ethanol. The tissue sections were incubated with the staining solution, which consisted of a 50% (w/vol) silver nitrate solution (Fisher Scientific, Nepean, Canada) and a 2% (w/vol) gelatin solution (J.T. Baker Chemical Co., Phillipsburg, NJ) mixed at a ratio of two to one, in a darkroom for 20 mins. The slides were then fixed with a 2% (w/vol) thiosulfate solution (BDH Inc., Toronto, Canada) for 60 seconds followed by dehydration and mounting. The number of hepatocytes with three or more silver staining nucleolus organizer regions (AgNORs) and the total number of hepatocytes were counted by two independent observers in five random microscopic fields ($\times 400$ magnification) per section. The proliferation index was calculated by dividing the number of hepatocytes with 3 or more AgNORs by the total number of hepatocytes per section. Results are expressed as means \pm SD of the total number of sections (one section per mouse) examined for each time point.

PCNA Immunohistochemistry. Cell proliferation was also determined with PCNA immunohistochemical staining as described previously (24) with few modifications. Briefly, paraffin-embedded liver samples sectioned at 5 μm were stained with a mouse anti-PCNA monoclonal antibody at a concentration of 2.5 $\mu\text{g}/\text{ml}$ (EMD Biosciences, Inc., La Jolla, CA) for 60 mins at room temperature. Tissue sections were counterstained with hematoxylin for detection of PCNA-negative nuclei and sections stained without primary antibody served as negative controls. The number of hepatocytes with PCNA-positive nuclei and the total number of hepatocytes were counted by two independent observers in five random microscopic fields ($\times 400$ magnification) per section. The proliferation index was calculated by dividing the number of hepatocytes with PCNA-positive nuclei by the total number of hepatocytes per section. Results are expressed as means \pm SD of the total number of sections (one section per mouse) examined for each time point.

Immunohistochemical Detection of MT. The subcellular localization of MT was determined with MT immunohistochemical staining as described previously (17).

Briefly, paraffin-embedded liver samples sectioned at 5 μm were stained with a mouse anti-MT serum E9 monoclonal antibody (DAKO Corporation, Carpinteria, CA) at 1:40 dilution overnight at 4°C. Tissue sections were counterstained with hematoxylin and sections stained without primary antibody served as negative controls.

Statistical Analyses. Statistical analysis of results was performed using the Student's two-tailed, unpaired *t* test for comparisons between groups. Differences were considered significant when $P < 0.05$ (group size, $n = 3$ or 6).

Results

Quantification of MT by the Cd-heme assay showed increasing levels of hepatic MT protein with time in WT mice after PH (Table 1). Hepatic MT levels in WT mice peaked at 24 hrs after PH, and were about 12 times higher than hepatic MT levels of control sham laparotomized mice. However, MT levels eventually declined to basal levels in WT mice by 60 hrs after PH. There was no change in the low basal levels of hepatic MT detected in MT-null mice, and they were still within the detection limit of the Cd-heme assay (Table 1).

Immunohistochemical staining for MT in WT mice showed localization of MT in both nucleus and cytoplasm of hepatocytes at 24 hrs after PH (Fig. 1A). At 36–60 hrs after PH or 48 hrs after sham laparotomy (control), MT was present mainly in the cytoplasm of hepatocytes in WT mice, which is similar to the cellular localization pattern for MT observed in adult mouse liver (Fig. 1B–D). There was no immunohistochemical detection of hepatic MT in livers of MT-null mice after PH or sham laparotomy.

The hepatic proliferation index was determined by two methods: AgNOR staining and PCNA immunohistochemical staining. There was no detectable proliferation of hepatocytes in WT and MT-null mice at 0, 5, and 15 hrs after PH, as measured by both AgNOR and PCNA staining techniques. The AgNOR staining technique showed about 10% (MT-null mice) and 15% (WT mice) of hepatocytes as proliferating at 48 hrs after sham laparotomy (control) (Fig. 2C). Proliferation index for WT mice was about 40% at 24 and 36 hrs, and peaked at about 55% at 48 hrs after PH. This was followed by a decline to about 40% by 60 hrs after PH (Fig. 2C). At every time point examined (24, 36, 48, and 60 hrs after PH), proliferation index for WT mice was significantly higher than that for MT-null mice ($P \leq 0.007$). Proliferation rates for both WT and MT-null mice at 48 hrs after PH were significantly higher than those for their respective controls at 48 hrs after sham laparotomy ($P \leq 0.016$). Hepatic proliferation index levels for MT-null mice were similar (about 18%–25%) at every time point examined after PH and did not change much during liver regeneration (Fig. 2C). At 24 hrs after PH, proliferation index for MT-null mice was similar to the low level (about 15%) observed for WT mice, which underwent sham laparotomy (control).

Table 1. Hepatic Metallothionein (MT) Protein Levels in Wild Type (WT) and MT-null Mice After Partial Hepatectomy (PH)^a

Time (hrs) after PH	MT levels ($\mu\text{g/g}$ liver tissue)	
	WT mice	MT-null mice
0	19.7 \pm 8.7 ^b	9.8 \pm 5.9
5	97.6 \pm 57.0	16.3 \pm 13.7
15	175.5 \pm 41.9 ^b	10.4 \pm 3.0
24	743.7 \pm 290.5 ^b	19.9 \pm 21.9
36	197.8 \pm 40.7 ^b	1.1 \pm 1.4
48	93.9 \pm 26.3	8.7 \pm 4.2
60	62.9 \pm 100.4	2.7 \pm 2.5
Sham laparotomy (control)	60.8 \pm 6.7	7.2 \pm 3.0

^a Hepatic MT levels were measured with the Cd-heme assay as described in Materials and Methods. Laparotomized mice served as sham-operated controls. The values shown are expressed as means \pm SD for 3 mice at 48 hrs after sham laparotomy, 3 mice at 5 and 15 hrs after PH, and 6 mice at 0, 24, 36, 48, and 60 hrs after PH.

^b Significantly different from the value of control sham laparotomized WT mice ($P < 0.05$).

The low hepatic proliferation index for both WT and MT-null mice at 48 hrs after sham laparotomy (control) was confirmed by PCNA immunohistochemical staining, and was about 6% (Fig. 3C). Proliferation index for WT mice was about 20% at 24, 36, and 60 hrs, and 45% at 48 hrs after PH (Fig. 3C). The results showed a sharp peak in proliferation index for WT mice at 48 hrs after PH. At 36, 48, and 60 hrs after PH, proliferation index for WT mice was significantly higher than that for MT-null mice ($P \leq 0.004$). Proliferation rates for both WT and MT-null mice at 48 hrs after PH were significantly higher than those for their respective controls at 48 hrs after sham laparotomy ($P \leq 0.004$). Hepatic proliferation index levels for MT-null mice were similar (about 10%–15%) at 24, 36, and 60 hrs, reaching a peak at 48 hrs after PH (Fig. 3C).

Discussion

The data presented here demonstrate an impairment of liver regeneration following PH in a MT-null mouse model. A previous study has shown low levels of hepatocyte proliferation after PH, as measured by PCNA immunoblotting, in rats treated with MT-directed antisense oligonucleotides. Although this technique reduced the levels of hepatic MT, these rats still had detectable levels of MT in the liver (25). Therefore, it is difficult to conclude any specific role for MT in liver regeneration from this study. In this study, we have used MT-null mice where both the major isoforms of MT (MT-I and MT-II) are deleted, and there was no positive immunohistochemical staining for hepatic MT in these mice. Moreover, hepatocyte proliferation after PH was measured by two methods. The data show that although cell proliferation occurred in both WT and MT-null mice after PH, the hepatocyte proliferation index for MT-null mice was much lower than that for WT mice. In addition, the

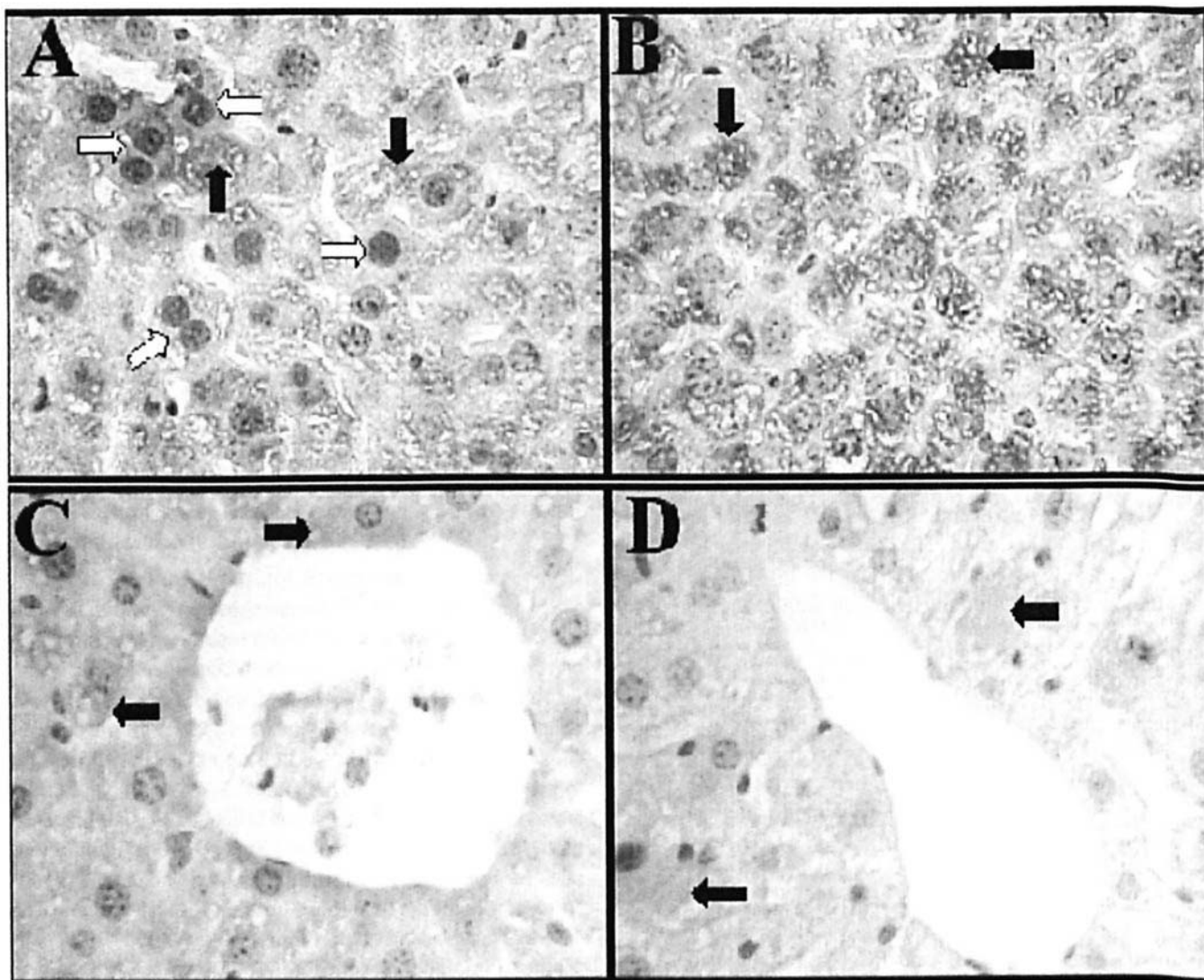


Figure 1. Effect of partial hepatectomy (PH) and hepatic regeneration on metallothionein (MT) protein expression in mouse liver. Immunohistochemical staining of wild-type mouse liver sections using a mouse MT-specific monoclonal antibody at (A) 24, (B) 36, (C) 48, and (D) 60 hrs after PH. Positive staining for MT in the nucleus (open arrows) and cytoplasm (closed arrows) of hepatocytes was detected at 24 hrs, while positive staining for MT was detected mainly in the cytoplasm at 36–60 hrs after PH. Magnification, $\times 400$.

induction of MT and its transient nuclear localization in hepatocytes of WT mice after PH suggest that MT, as a zinc storage protein, could accumulate zinc in the nucleus during rapid cellular growth.

We have used both AgNOR staining and PCNA immunohistochemical staining to assess hepatocyte proliferation because these two techniques can measure markers at different stages of the cell cycle. The AgNOR technique stains the nucleolus organizer region (NOR), which is the region of a chromosome containing the major ribosomal RNA (rRNA) genes (26). Morton *et al.* (27) demonstrated that the AgNOR stain intensity directly reflects rRNA gene transcriptional activity as measured by tritiated uridine incorporation into 18S and 28S rRNA in cultured fibroblasts. Thus, it was concluded that the number of AgNORs reflects the level of rRNA synthesis, which is

known to increase in response to an increase in mitotic rate. During M phase of the cell cycle, the chromosomes begin to rearrange themselves and eventually separate, as seen in anaphase. Therefore, the presence of multiple small AgNORs is believed to be indicative of M phase, whereas during quiescence, the individual AgNORs coalesce into one large AgNOR (28). Because PCNA is a component of the DNA polymerase δ machinery, immunostaining for PCNA is specific to S phase of the cell cycle. Because AgNOR and PCNA are indicative of different stages of the cell cycle, proliferation index as measured by these two techniques showed different values. However, they showed similar patterns, and at 48 hrs after PH, proliferation index measured with both PCNA and AgNOR techniques was at a maximum. This supports the findings that DNA replication and mitosis peak at about 44 hrs after PH in mice (29).

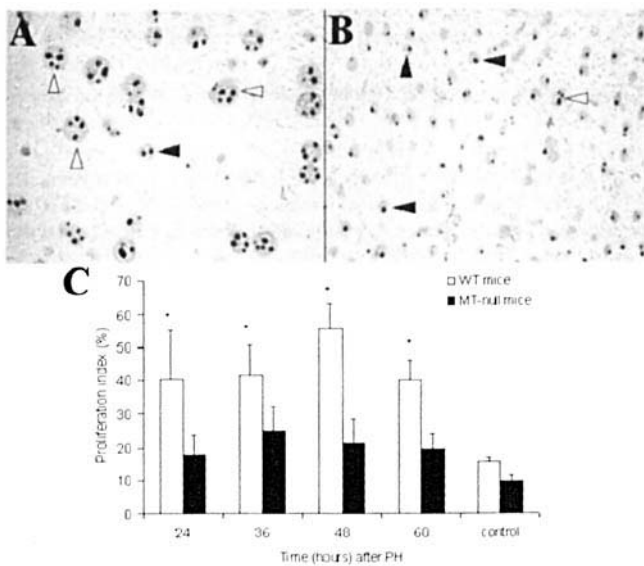


Figure 2. Argyrophilic nucleolar organizing region (AgNOR) staining of (A) wild-type and (B) metallothionein (MT)-null mouse liver sections at 48 hrs after partial hepatectomy (PH). Proliferating hepatocytes are those with enlarged nuclei containing three or more AgNORs (open arrowheads) and quiescent hepatocytes are those with smaller nuclei containing only one or two AgNORs (closed arrowheads). Magnification, $\times 400$. (C) Hepatic proliferation index in wild-type and MT-null mice at different time points after PH as determined by AgNOR staining. Control mice represent proliferation index at 48 hrs after sham laparotomy. Data are expressed as means \pm SD for groups of six mice at 24, 36, 48, and 60 hrs after PH and three mice for the control group. *Significantly different from the value of the MT-null mice at same time points after PH ($P < 0.05$).

There are many possible explanations on impaired hepatic regeneration in MT-null mice after PH as compared to WT mice. Because of extensive TNF- α signaling and the increased metabolic activity of hepatocytes to maintain homeostasis after PH, the levels of reactive oxygen species (ROS) are augmented during liver regeneration (29). Because the rapidly proliferating cells of the regenerating liver are extremely susceptible to oxidant damage, the generation of ROS can result in cell cycle arrest. Studies have shown the induction of uncoupling protein-2 (UCP-2) in response to TNF- α mediated mitochondrial oxidant production in regenerating rodent liver after PH (30, 31). UCP-2 is an inner mitochondrial membrane protein that can act as a channel for protons, thereby dissipating the electrochemical gradient and decreasing oxidant production. MT may also play a role in reducing ROS levels during the regenerative process after PH, but by a different mechanism. For instance, by scavenging excess of ROS, MT may modulate oxidative stress-induced cell cycle arrest and apoptosis, thereby allowing cell proliferation during hepatic regeneration. An *in vivo* study using MT-overexpressing transgenic mice showed that hepatic MT could protect against alcoholic liver injury through inhibition of oxidative stress (32). Although studies have shown that they are normal with similar growth patterns as WT mice, MT-null mice are more sensitive to oxidative stress-inducing agents such as cadmium, strepto-

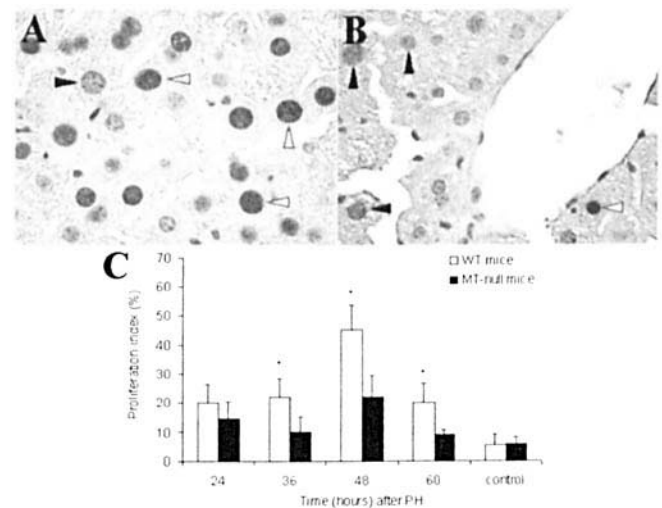


Figure 3. Immunohistochemical staining of PCNA with a mouse PCNA-specific monoclonal antibody in (A) wild-type and (B) metallothionein (MT)-null mouse liver sections at 48 hrs after partial hepatectomy (PH). Proliferating hepatocytes are stained positive for PCNA (open arrowheads) and quiescent hepatocytes are negative for PCNA (closed arrowheads). Magnification, $\times 400$. (C) Hepatic proliferation index in wild-type and MT-null mice at different time points after PH as determined by immunohistochemical staining for PCNA. Control mice represent proliferation index at 48 hrs after sham laparotomy. Data are expressed as means \pm SD for groups of six mice at 24, 36, 48, and 60 hrs after PH and three mice for the control group. *Significantly different from the value of the MT-null mice at same time points after PH ($P < 0.05$).

zotocin, carbon tetrachloride, and acetaminophen than WT mice (33–36). However, there are no reports on impairment of cellular growth in MT-null mice.

During the initiation phase of liver regeneration, quiescent hepatocytes are primed to respond to growth factors. During this priming phase, the hepatocytes enter into a state of replicative competence. In IL-6 null mice, it has been established that IL-6 plays a pivotal role in the induction of hepatic MT after PH (37). Because IL-6 is one of the main cytokines implicated in the priming phase of liver regeneration, MT may be involved in the priming of hepatocytes after PH. In addition, previous *in vitro* studies have shown that a translocation of MT from the cytoplasm to the nucleus occurs during S through G₂-M phases of the cell cycle (38, 39). Furthermore, the transient nuclear localization of MT after PH, as shown in this study, supports a potential role for MT as a zinc donor to various transcription factors during liver regeneration. Thus, MT may play a role in the priming of hepatocytes after PH by donating zinc to nuclear zinc finger transcription factors and metallo-enzymes (DNA polymerase, RNA polymerase) involved in the regulation of DNA synthesis. Indeed, many proteins depend on zinc for proper folding, and essential structural and catalytic stability. Also, *in vitro* studies have shown that oxidized glutathione (GSSG) can enhance the transfer rate of zinc from MT to metallo-proteins (40, 41). Because of augmented ROS levels after PH, a low GSH/GSSG ratio may occur in regenerating liver (42). Thus, the

elevated GSSG levels may facilitate release of zinc ions from MT, which is a zinc and copper storage protein, and thereby increase the availability of zinc ions for various zinc requiring metallo-proteins.

The positive role of MT in liver regeneration may have clinical applications. Because there is remarkable similarity between the process of hepatic regeneration in laboratory animals and humans (43), induction of MT could have the potential to augment liver regeneration in patients after surgical resection (i.e., transplantation, tumor removal, etc.). In summary, we have demonstrated a positive role for MT in liver regeneration after PH, using a MT-null mouse model. The mechanisms involved in liver regeneration have been studied in various laboratories but further studies are required to understand the exact role of MT in various stages of cellular regeneration.

We thank Sean Jiang and Weihua Liu for their technical assistance in this work.

1. Michalopoulos GK, DeFrances MC. Liver regeneration. *Science* 276:60–66, 1997.
2. Zimmermann A. Liver regeneration: the emergence of new pathways. *Med Sci Monit* 8:RA53–63, 2002.
3. Koniaris LG, McKillop IH, Schwartz SI, Zimmers TA. Liver regeneration. *J Am Coll Surg* 197:634–659, 2003.
4. Zeng J, Heuchel R, Schaffner W, Kagi JH. Thionein (apo-metallothionein) can modulate DNA binding and transcription activation by zinc finger containing factor Sp1. *FEBS Lett* 279:310–312, 1991.
5. Zeng J, Vallee BL, Kagi JH. Zinc transfer from transcription factor IIIA fingers to thionein clusters. *Proc Natl Acad Sci USA* 88:9984–9988, 1991.
6. Cano-Gauci DF, Sarkar B. Reversible zinc exchange between metallothionein and the estrogen receptor zinc finger. *FEBS Lett* 386:1–4, 1996.
7. Roesijadi G, Bogumil R, Vasak M, Kagi JH. Modulation of DNA binding of a tramtrack zinc finger peptide by the metallothionein-thionein conjugate pair. *J Biol Chem* 273:17425–17432, 1998.
8. Udom AO, Brady FO. Reactivation in vitro of zinc-requiring apoenzymes by rat liver zinc-thionein. *Biochem J* 187:329–335, 1980.
9. Quesada AR, Byrnes RW, Krezoski SO, Petering DH. Direct reaction of H₂O₂ with sulfhydryl groups in HL-60 cells: zinc-metalllothionein and other sites. *Arch Biochem Biophys* 334:241–250, 1996.
10. Jimenez I, Gotteland M, Zarzuelo A, Uauy R, Speisky H. Loss of the metal binding properties of metallothionein induced by hydrogen peroxide and free radicals. *Toxicology* 120:37–46, 1997.
11. Cai L, Cherian MG. Zinc-metalllothionein protects from DNA damage induced by radiation better than glutathione and copper- or cadmium-metalllothioneins. *Toxicol Lett* 136:193–198, 2003.
12. Wong KL, Klaassen CD. Isolation and characterization of metallothionein, which is highly concentrated in newborn rat liver. *J Biol Chem* 254:12399–12403, 1979.
13. Brady FO. The physiological function of metallothionein. *Trends Biochem Sci* 7:143–145, 1982.
14. Waalkes MP, Goering PL. Metallothionein and other cadmium-binding proteins: recent developments. *Chem Res Toxicol* 3:281–288, 1990.
15. Nartey NO, Banerjee D, Cherian MG. Immunohistochemical localization of metallothionein in cell nucleus and cytoplasm of fetal human liver and kidney and its changes during development. *Pathology* 19:233–238, 1987.
16. Chan HM, Cherian MG. Ontogenic changes in hepatic metallothionein isoforms in prenatal and newborn rats. *Biochem Cell Biol* 71:133–140, 1993.
17. Lau JC, Cherian MG. Developmental changes in hepatic metallothionein, zinc, and copper levels in genetically altered mice. *Biochem Cell Biol* 76:615–623, 1998.
18. Tohyama C, Suzuki JS, Hemelraad J, Nishimura N, Nishimura H. Induction of metallothionein and its localization in the nucleus of rat hepatocytes after partial hepatectomy. *Hepatology* 18:1193–1201, 1993.
19. Tsujikawa K, Suzuki N, Sagawa K, Itoh M, Sugiyama T, Kohama Y, Otaki N, Kimura M, Mimura T. Induction and subcellular localization of metallothionein in regenerating rat liver. *Eur J Cell Biol* 63:240–246, 1994.
20. Theocharis SE, Margeli AP, Skaltsas SD, Spiliopoulou CA, Koutselinis AS. Induction of metallothionein in the liver of carbon tetrachloride intoxicated rats: an immunohistochemical study. *Toxicology* 161:129–138, 2001.
21. Greene AK, Puder M. Partial hepatectomy in the mouse: technique and perioperative management. *J Invest Surg* 16:99–102, 2003.
22. Onosaka S, Cherian MG. The induced synthesis of metallothionein in various tissues of rat in response to metals. *Toxicology* 22:91–101, 1981.
23. Ploton D, Bobichon H, Adnet J. Ultrastructural localization of NOR in nucleoli of human breast cancer tissues using a one-step Ag-NOR staining method. *Biol Cell* 43:229–232, 1982.
24. Rai RM, Yang SQ, McClain C, Karp CL, Klein AS, Diehl AM. Kupffer cell depletion by gadolinium chloride enhances liver regeneration after partial hepatectomy in rats. *Am J Physiol* 270:G909–G918, 1996.
25. Arora V, Iversen PL, Ebadi M. Manipulation of metallothionein expression in the regenerating rat liver using antisense oligonucleotides. *Biochem Biophys Res Commun* 246:711–718, 1998.
26. Schwarzacher HG, Wachtler F. Nucleolus organizer regions and nucleoli: cytological findings. In: Stahl A, Luciani JM, Vagner-Capodano AM, Eds. *Chromosomes Today*. London: Allen and Unwin, Vol 9, pp252–260, 1987.
27. Morton C, Brown J, Holmes W, Nance W, Wolf B. Stain intensity of human nucleolus organizer region reflects incorporation of uridine into mature ribosomal RNA. *Exp Cell Res* 145:405–413, 1983.
28. Goessens G, Thiry M, Lepoint A. Relations between nucleoli and nucleolus-organizing regions during the cell cycle. In: Stahl A, Luciani JM, Vagner-Capodano AM, Eds. *Chromosomes Today*. London: Allen and Unwin, Vol 9, pp261–271, 1987.
29. Fausto N. Liver Regeneration. *J Hepatol* 32:19–31, 2000.
30. Lee FY, Li Y, Zhu H, Yang S, Lin HZ, Trush M. Tumor necrosis factor increases mitochondrial oxidant production and induces expression of uncoupling protein-2 in the regenerating rat liver. *Hepatology* 29:677–687, 1999.
31. Horimoto M, Fulop P, Derdak Z, Wands JR, Baffy G. Uncoupling protein-2 deficiency promotes oxidant stress and delays liver regeneration in mice. *Hepatology* 39:386–392, 2004.
32. Zhou Z, Sun X, Kang Y. Metallothionein protection against alcoholic liver injury through inhibition of oxidative stress. *Exp Biol Med* 227:214–222, 2002.
33. Masters BA, Kelly EJ, Quaife CJ, Brinster RL, Palmiter RD. Targeted disruption of metallothionein I and II genes increases sensitivity to cadmium. *Proc Natl Acad Sci USA* 91:584–588, 1994.
34. Apostolova MD, Choo KH, Michalska AE, Tohyama C. Analysis of the possible protective role of metallothionein in streptozotocin-induced diabetes using metallothionein-null mice. *J Trace Elem Med Biol* 11:1–7, 1997.
35. Satoh M, Tohyama C. Susceptibility to metals and radical-inducing chemicals of metallothionein-null mice. In: Klaassen CD, Ed. *Metallothionein IV*. Boston: Birkhauser, pp541–546, 1999.
36. Liu J, Liu YP, Hartley D, Klaassen CD, Shehin-Johnson SE, Lucas A, Cohen SD. Metallothionein-I/II knockout mice are sensitive to

- acetaminophen-induced hepatotoxicity. *J Pharmacol Exp Ther* 289:580–586, 1999.
37. Molotkov A, Nishimura N, Masahiko S, Tohyama C. Role of IL-6 in the induction of hepatic metallothionein in mice after partial hepatectomy. *Life Sci* 66:963–970, 2000.
38. Cherian MG, Apostolova MD. Nuclear localization of metallothionein during cell proliferation and differentiation. *Cell Mol Biol* 46:347–356, 2000.
39. Apostolova MD, Cherian MG. Delay of M-phase onset by aphidicolin can retain the nuclear localization of zinc and metallothionein in 3T3-L1 fibroblasts. *J Cell Physiol* 183:247–253, 2000.
40. Maret W. Oxidative metal release from metallothionein via zinc- thiol/ disulfide interchange. *Proc Natl Acad Sci USA* 91:237–241, 1994.
41. Jiang LJ, Maret W, Vallee BL. The glutathione redox couple modulates zinc transfer from metallothionein to zinc-depleted sorbitol dehydrogenase. *Proc Natl Acad Sci USA* 95:3483–3488, 1998.
42. Vendemiale G, Guerrieri F, Grattagliano I, Didonna D, Muolo L, Altomare E. Mitochondrial oxidative phosphorylation and intracellular glutathione compartmentation during rat liver regeneration. *Hepatology* 21:1450–1454, 1995.
43. Fausto N. Liver regeneration: from laboratory to clinic. *Liver Transpl* 7:835–844, 2001.